Biochimica et Biophysica Acta, 985 (1989) 239–247
Elsevier

BBAMEM 74602

Pore-forming properties of the adsorption protein of filamentous phage fd

Gabriele Glaser-Wuttke, Jutta Keppner and Ihab Rasched

Fakultät für Biologie der Universität Konstanz, Konstanz (F.R.G.)

(Received 2 May 1989)

Key words: Pore protein; Adsorption protein; Phage fd

The gene 3-encoded adsorption protein (g3p) of filamentous phage fd has been purified to homogeneity by using high-performance liquid chromatography. Removal of SDS from the SDS-solubilized g3p results in spontaneous oligomerization of the g3p. Reconstitution into artificial lipid bilayer membranes shows that the oligomer forms large aqueous pores that remain open for seconds and are insensitive to changes in membrane potential. The estimated diameter of the pores suggest that they are large enough to allow passage of phage single-stranded DNA. The implications of these findings for phage infection are discussed.

Introduction

Although much effort has been dedicated to the study of filamentous coliphages over the past 20 years some basic features of the viral life cycle are still poorly understood. One of them is the way in which the DNA of infecting phage overcomes the outer and cytoplasmic membranes of *Escherichia coli* [1].

The closely related F-specific filamentous (Ff) phages fd, f1 and M13 infect *E. coli* strains which harbour the conjugative F-plasmid. Infection is initiated by the binding of one end of the phage to the tip of the F-pilus [2]. This binding is mediated by the N-terminal part of the gene 3-encoded viral adsorption protein g3p [3] which protrudes as a knob-like structure from one end of the phage filament. Electron microscopy visualizes three of these knobs on each particle [4]. G3p is 406 amino acids long; a hydrophobic stretch of 23 amino acids near its carboxy-terminus mediates its binding to the phage coat [3]. This region is also necessary for proper anchoring of newly synthesized g3p in the host inner membrane [5,6].

It is postulated that bound phage is brought to the cell surface by progressive depolymerization of the pilus into the membrane [7–9]. There the DNA is released into the cytoplasm and the capsid proteins integrate into the membrane [10–12].

Transport of the DNA across the membranes requires both bacterial and phage proteins. *E. coli* mutated in the chromosomal genes tolA, tolQ or tolR do not allow transport of filamentous phage DNA into the cytoplasm [13,14]. Mutations in these tol-genes (and in tolB) also render cells tolerant to group A colicins (A, E1, E2, E3, K, N) [13,15]. As the products of the tolQRAB gene cluster are associated with the cell membrane it was concluded, that these proteins are necessary for the translocation of both filamentous phage DNA and group A colicins across the cytoplasmic membrane [13]. Translocation of filamentous phage DNA also requires the viral adsorption protein which is supposed to interact with the tolQRA products [14].

Recent evidence suggests that g3p also participates in transport functions through the outer membrane [16]. The 372 N-terminal codons of g3p were fused in frame to sequences encoding the C-terminal third of colicin E3. This portion of ColE3 harbours its RNase activity which is responsible for killing of susceptible cells. It is, however, devoid of the central domain of native colicin which harbours the receptor-binding function, as well as an N-terminal domain which has been implicated in translocation of the colicin through the outer membrane [17–19]. In contrast to native colicin which kills $btuB^+$-cells, the g3p-ColE3 hybrid protein kills only F^+-cells. This demonstrates that translocation of the RNase ac-

Abbreviations: ColE3, colicin E3; Ff, F-specific filamentous; g3p, gene 3 protein (adsorption protein); g8p, gene 8 protein (major coat protein); nS, nanoSiemens (1 S = 1 A/V); SDS, sodium dodecyl sulfate; DTBP, dimethyl-3,3′-dithiobispropionimidate dihydrochloride; FPLC, fast protein liquid chromatography; V_e, elution volume.

Correspondence: I. Rasched, Fakultät für Biologie der Universität Konstanz, D-7750 Konstanz, F.R.G.

tivity into the cytoplasm is mediated by g3p. Thus, g3p is capable of confering both a receptor-binding function (to the F-pilus) and a transport function (through the outer membrane) to the truncated ColE3, thereby restoring its capacity to overcome the host outer membrane barrier. (Further transport of the fusion protein is thought to follow the pathway normally used by colicins rather than the Ff-specific pathway [16].)

The role of g3p in translocation of both the ColE3-moiety (of the hybrid protein) and the phage DNA in filamentous phage infection implies at least a transient insertion of g3p or a fragment thereof into the outer membrane. An original investigation concerning the fate of the phage g3p in infected cells showed that a g3p-fragment enters the cell with the phage DNA [11]. More detailed cell fractionation studies of infected cells revealed the presence of g3p-fragments in both the cytoplasmic membrane and the periplasm, in the outer membrane, however, the integral g3p was found [12].

In accordance with Kornberg [20] the latter observation led us to hypothesize that part of the role of the adsorption protein in filamentous phage infection is the formation of a membrane pore, thus allowing penetration of the charged DNA-molecule through the lipid bilayer of the membrane. This paper supports this idea by demonstrating that g3p displays pore-forming properties in vitro. We also present evidence that an oligomeric form of g3p is the pore-forming entity. Furthermore, the amino acid sequence of g3p was analyzed by secondary structure prediction methods in a search for protein segments likely to interact with membranes and to form the pore.

Materials and Methods

Growth and purification of bacteriophage fd

Wild-type fd virus was grown in LB-medium [21] supplemented with glucose (0.05%) using *E. coli* K37 (Hfr C, sup D) as host cells. At a density of $1 \cdot 10^8$ cells/ml, the culture was infected with fd phages (multiplicity of infection: 1). After growth over night, the cells were spun down and the virus was precipitated from the supernatant as described by Yamamoto [22]. The recovered phages were resuspended in 100 ml of 10 mM sodium citrate (pH 7.6) (citrate solution), 0.1% Sarkosyl NL-97, and stirred slowly at room temperature for 30 min. Reprecipitation of the phage was performed with 5% poly(ethylene glycol) 6000 and 0.5 M NaCl for 2 h at 4° C. The phage was collected by centrifugation and dissolved in 10 to 20 ml of citrate solution. The phage was further purified by sedimentation in a CsCl-density gradient (4.7 g CsCl in 10 ml citrate solution) for 20 h at 4° C at 145 000 × *g*. The phage band was collected and dialyzed against citrate solution. The concentrations of phage were determined photometrically at 269 nm using an absorption coefficient of 3.84 $mg^{-1} \cdot cm^{-2}$ [23]. Purified phage was stored frozen at −20° C until further use.

Isolation of g3p

Fd-phage (about 10 mg/ml) in citrate solution was dissociated with SDS in a final concentration of 1% (w/v). The pH of this solution was adjusted to 5.4 by adding 1 M HCl. Up to 200 µl of dissociated virus were loaded onto a Superose 12 column (1.0 cm i.d. × 30 cm; Pharmacia). The column was eluted using 5 mM citric acid (pH3), 50 mM Na_2SO_4, 1% SDS, as eluent. Peaks were collected and dialyzed exhaustively into water.

Reconstitution and purification of oligomeric g3p

Dialyzed g3p was lyophilized; the lyophilized residue was resuspended in 5 mM citric acid (pH 3), 0.2 M Na_2SO_4, 1% SDS to give a final g3p concentration of 0.8 mg/ml. Solubilization of g3p was accomplished by sonication on ice using a Branson sonifier with a microtip in pulsed position (timer, 3 min; %duty cycle, 50; output control, 7). This concentrated A-protein solution was rechromatographed on the Superose 12 column. Then, β-mercaptoethanol in a final concentration of 1% was added.

HPLC-apparatus

The chromatographic equipment consisted of a 2150 HPLC pump (LKB), and a 2154 loop injection valve (LKB). Absorption was monitored at 206 nm using a 2158 Uvicord SD (LKB) or a variable wavelength monitor 720 LC (Kontron) and recorded using a 3390A integrator (Hewlett-Packard). Peaks were collected using the peak-slope detection system of a 2211 Super-Rac fraction collector (LKB).

SDS-polyacrylamide gel electrophoresis

Slab-gel electrophoresis was performed in the presence of 0.1% SDS according to Laemmli [24] with the following modifications: The separation gel contained 15% acrylamide and 0.09% *N,N'*-methylene(bisacrylamide). The stacking gel consisted of 5% acrylamide and 0.13% bisacrylamide. Samples were boiled in 4% SDS under reducing conditions for 5 min unless otherwise indicated. Staining was with the silver nitrate method [25].

Cross-linking of phage-associated g3p

G3p in native fd phages was cross-linked using the cleavable imidoester DTBP (dimethyl-3,3'-dithiobispropionimidate dihydrochloride; Pierce). 1.0 ml of fd-phages (12 mg/ml) were dialyzed thoroughly into 0.2 M triethanolamine-HCl (pH 8.5), diluted with this buffer to give a final concentration of 1.3 mg/ml. 48 mg of DTBP were added corresponding to a 10-fold molar excess above all primary amino-groups of the phage. After 2.5 h of incubation at room temperature, the

reaction mixture was dialyzed into plenty of water. Then, the volume of the sample was reduced to 1.0 ml by incubation in poly(ethylene glycol) 20000 (Serva) and buffered with sodium citrate in a final concentration of 10 mM. Dissociation of this cross-linked phage was as described except that the SDS-concentration used was 5% (w/v). The phage DNA was sedimented at $110000 \times g$ in 4–5 h. Aliquots of the resulting supernatant were chromatographed on the Superose 12 column.

Reductive cleavage of the cross-linker was brought about by the addition of dithiothreitol to the phage protein supernatant in a final concentration of 0.65 M and a subsequent 30 min incubation period at 37 °C.

Incorporation of g3p into planar lipid bilayers and conductance measurements

Artifical lipid bilayer membranes were obtained as described previously [26] from a 1–2% (w/v) solution of oxidized cholesterol in *n*-decane (purum grade: Fluka, Buchs, Switzerland). The chamber used for bilayer formation was made from Teflon. The circular hole separating the two aqueous compartments (each about 5 ml volume) had an area of 0.1 mm^2. The aqueous phase consisted of 1.0 M KCl. The protein was added from stock solutions containing 1% β-mercaptoethanol and up to 1% SDS to the aqueous phase either before membrane formation or after the membrane had completely turned black. For the electrical measurements calomel electrodes with salt bridges were inserted into the aqueous compartments on both sides of the membrane. A Keithley 427 current amplifier was used for the single channel experiments. The boosted signal was monitored by a Tektronix 5115 storage oscilloscope and recorded using a strip-chart recorder.

Results

Structural comparison of g3p and pore-forming proteins

The pore-forming proteins (porins) in the outer membrane of gram-negative bacteria share a number of structural features: Their molecular masses range between 30 and 50 kDa, they are acidic proteins containing about 20 mol% charged amino acids and a total of almost 50% polar amino acids [27]. A comparison of porins to g3p reveals that the adsorption protein of filamentous phage fd displays these structural characteristics as well. Moreover, its overall amino acid composition is remarkably similar to those of various porins (Table I) [28].

Another structural theme common to membrane pores and channels is their stable insertion into the membrane. This is usually accomplished by bundles of membrane-spanning α-helices or β-strands [30]. However, apart from the C-terminal membrane anchor domain, the primary structure of g3p does not contain any further hydrophobic stretches which are long enough to span a membrane (Fig. 1A). Therefore, we used structure prediction to reveal putative membrane-spanning amphipathic β-strands. Such amphipathic β-strands have also been predicted for the *E. coli* porin, OmpF, and led to suggest a detailed folding model for OmpF in the membrane. In this model the hydrophobic sides of the β-strands are oriented towards the lipids, whereas their hydrophilic sides face the aqueous pore interior in the centre of the porin trimer [30], thus accounting for the incorporation of a high percentage of hydrophilic residues into the membrane. Due to their aggregation into trimers around a central aqueous pore the lipid/protein interface per monomer is even further reduced.

As shown in Fig. 1B, the g3p amino acid sequence does contain several putative membrane-spanning domains. Thus g3p fulfills the structural requirements needed to form a membrane pore.

TABLE I

Amino acid composition of the g3p of phage fd compared to that of various porins

	g3p [a]	OmpF [b]	OmpC [b]	PhoE [b]
Molecular mass (kDa)	42.8	37.1	38.3	36.8
Polarity index [c] (mol%)	43.7	44.4	47.4	50.1
Amino acid (mol%)				
Asp	5.9	7.9	9.2	9.4
Asn	7.2	8.9	9.0	8.2
Thr	6.4	6.2	6.9	7.0
Ser	7.9	4.7	4.6	5.5
Glu	6.4	4.1	4.0	4.2
Gln	3.7	3.8	5.3	4.9
Pro	6.2	1.2	0.9	0.9
Gly	16.8	14.1	13.6	10.9
Ala	6.9	8.5	6.9	8.2
Cys	2.0	0.0	0.0	0.0
Val	4.9	6.8	6.1	3.6
Met	1.7	0.9	0.9	2.1
Ile	2.2	3.5	2.9	3.9
Leu	4.7	5.9	6.4	6.4
Tyr	5.2	8.5	8.4	6.7
Phe	4.9	5.6	5.5	6.4
Trp	1.0	0.6	1.2	0.9
Lys	3.5	5.3	4.3	7.0
His	0.5	0.3	0.3	0.3
Arg	2.2	3.2	3.8	3.6

[a] Beck and Zink [28]
[b] Mizuno et al. [29].
[c] Capaldi and Vanderkooi [43].

Purification of g3p

The protein coat of phage fd is composed of five different proteins. G3p and 3 other minor coat proteins are present in only 3–5 copies each in the coat, whereas the major coat protein (g8p, B-protein) accounts for

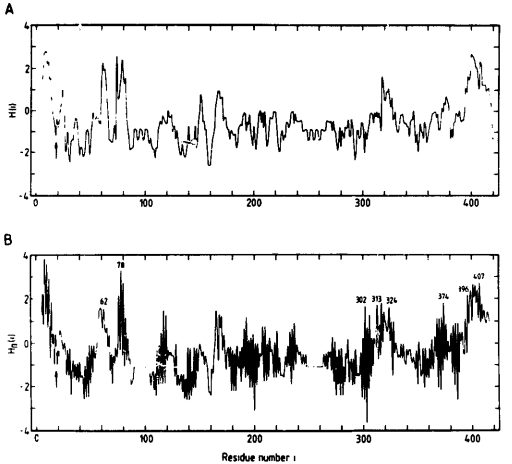

Fig. 1. Structure prediction plots for g3p against the amino acid residue position i (including signal peptide 1–18). The arrow marks the beginning of mature g3p. (A) Average hydrophobicity, $H(i)$, per seven residues according to the method of Kyte and Doolittle [44]. A membrane-spanning α-helix is predicted if $H(i) > 1.6$ over a region of about 20 residues. (B) Mean hydrophobicity $H_\beta(i)$ of one side of an amphipathic membrane-spanning β-strand around residue i [30]. An amphipathic β-strand is identified by an oscillation of $H_\beta(i)$ with a period of two residues, i.e. $H_\beta(i) > 1.6$ and $H_\beta(i \pm 1) \ll 1.6$. The numbers refer to residue i in the middle of a predicted amphipathic β-strand comprising 9 or 10 residues. A similar approach for the prediction of amphipathic α-helices [30] reveals two amphipathic α-helices which are centred around residue 317 and 402, respectively.

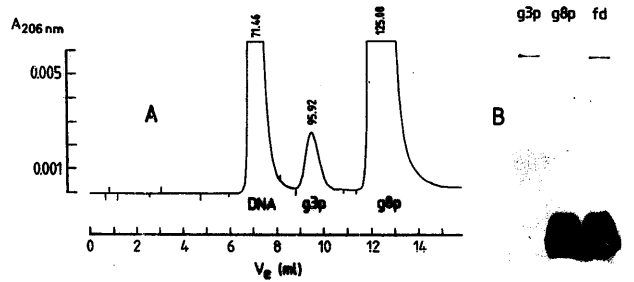

Fig. 2. Purification of g3p using a Superose 12 column. (A) Elution profile of 120 μg dissociated fd-phage eluted at a flow-rate of 0.1 ml/min. The numbers above the peaks are retention times (min). (B) Electrophoretic analysis of g3p and g8p purified as in (A). 25 ng of g3p and 1 μg of g8p were applied to lane g3p and g8p, respectively. An aliquot of fd-phage (2.5 μg) was applied to lane fd and displays the equivalent of about 25 ng g3p and about 2.5 μg g8p.

about 99% of the protein mass of the phage coat. Solubilization of the extremely insoluble coat proteins requires the use of a detergent or denaturant [31]. Because published procedures to purify g3p are tedious and time-consuming [31–33], we developed a gel-filtration technique using the fact that the molecular mass of g3p (42.6 kDa) is much higher than that of any other coat protein (12–3.5 kDa) [34–36]. This technique allows a one-step purification of homogeneous g3p within less than 2 h. Furthermore, detection of the phage components at 206 nm allows optical monitoring of g3p, thus radioactive labeling was superfluous. (Detection of g3p at 280 nm is generally not possible due to its minute amount in the phage coat.)

Fig. 2A shows a standard fractionation of SDS-dissociated fd-phage on a Superose 12 column. In order of their elution the 3 peaks were identified as phage DNA, g3p and g8p, the surplus of g8p superimposing the other minor coat proteins. Homogeneity of the purified g3p was revealed by electrophoresis followed by silver nitrate staining (Fig. 2B) and also by rechromatography. The elution profile of an aliquot (200 µl) of the g3p peak fraction which was reinjected into the FPLC-system showed a single peak (results not shown). Furthermore, if subjected to amino acid analysis, the amino acid composition of the purified g3p was in agreement with its theoretical composition deduced from the DNA-sequence.

However, if the g3p-containing fractions were dialyzed against water, lyophilized and rechromatographed thereafter, the elution profile displayed two distinct peaks, the retention time of the second peak being identical with that of the original g3p-peak (Fig. 3). Analysis by electrophoresis (7.5% gel) confirmed that both peaks consisted of g3p. They showed a single band

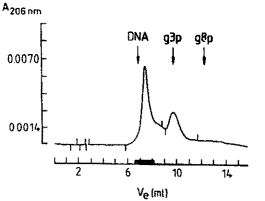

Fig. 3. Reconstitution and purification of oligomeric g3p. G3p purified as in Fig. 2A was concentrated by lyophilization after the removal of SDS by dialysis. 3.5 µg of the solubilized lyophilisate (see Materials and Methods) were loaded onto a Superose 12 column and eluted at a flow rate of 0.2 ml/min. Under these conditions, the components of dissociated fd-phages eluted at the positions indicated by arrows. The peak denoted by the bar was identified as g3p by electrophoresis. It will be referred to as 'oligomeric g3p'.

each, both bands having the same electrophoretic mobility as g3p originating from coelectrophoresed fd-phage. Hence, dialysis and/or lyophilization caused monomeric g3p to associate to an oligomeric form which was persistent in the 1% SDS-containing column buffer but dissociated into monomers upon electrophoresis. This was also true if the electrophoresis was under non-reducing conditions or if the g3p-oligomer had not been boiled prior to electrophoresis (results not shown). Thus, there are no interchain disulfide bridges in the g3p-oligomer.

Membrane conductance measurements

Both monomeric and oligomeric g3p were subjected to single channel experiments which judge the pore-for-

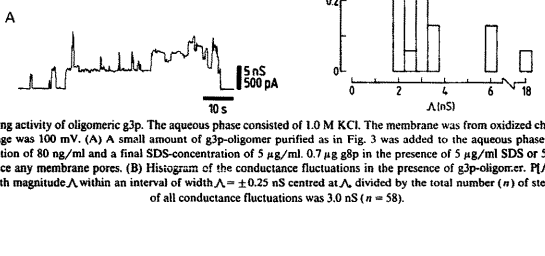

Fig. 4. Pore-forming activity of oligomeric g3p. The aqueous phase consisted of 1.0 M KCl. The membrane was from oxidized cholesterol/*n*-decane. The applied voltage was 100 mV. (A) A small amount of g3p-oligomer purified as in Fig. 3 was added to the aqueous phase resulting in a final protein concentration of 80 ng/ml and a final SDS-concentration of 5 µg/ml. 0.7 µg g8p in the presence of 5 µg/ml SDS or 5 µg/ml SDS on its own did not induce any membrane pores. (B) Histogram of the conductance fluctuations in the presence of g3p-oligomer. P[Λ] is the number of observed steps with magnitude Λ within an interval of width $\Lambda = \pm 0.25$ nS centred at Λ, divided by the total number (n) of steps. The mean value of all conductance fluctuations was 3.0 nS ($n = 58$).

ming capability of a protein from its ability to cause rectangular current pulses across a membrane at a given transmembrane potential.

The addition of oligomeric g3p to the aqueous phase surrounding a lipid bilayer resulted in a stepwise change in membrane current (Fig. 4A), irrespective of the polarity and the size of the voltage (10–150 mV) applied. The occurrence of these quantal leaps was specific for the presence of g3p. Detergent alone or similar concenirations of g8p did not produce these effects. On an average, the current steps had a single-channel conductance of 3.0 nS (Fig. 4B). Their lifetime was in the order of seconds, and they were directed both upwards and downwards. However, the current traces were rather noisy and the noise level increased with the number of pores in the membrane. Pore-formation usually occurred within minutes after protein addition to the aqueous phase.

In contrast, with monomeric g3p there was an initial lag of at least an hour after protein addition before pore-formation could be observed. Thereafter, the frequency of pore events would increase with time. However, the observation of pores was hampered by the effect of monomeric g3p on membrane stability. Frequently, the membrane broke within seconds after g3p addition. In general, more protein was necessary for conductivity measurements; the final concentrations of monomeric and oligomeric g3p in the experiments ranged from 50–400 ng/ml and 0.05–80 ng/ml, respectively. Finally, the pore size distribution was broader and the average single-channel conductance in 1 M KCl was only 2.1 nS (Fig. 5). Occasionally, conductance steps of 0.2 nS were also observed. (The latter pore could not be investigated in detail because of the abundance of the larger pore.)

These differences in pore-formation between monomeric and oligomeric g3p led us to conclude that the oligomeric g3p is the prepackaged pore-forming entity which upon addition to the aqueous phase can be readily inserted into the membrane. Monomeric g3p, however, does not seem to have pore-forming properties by itself. This view is supported by two lines of evidence. First, monomeric g3p greatly destabilizes the membranes. This indicates that it is membrane-active. Its interaction with the membrane, however, results in a general disturbance of the bilayer structure, rather than in its own stable insertion into the membrane. Second, current steps could only be seen after a long delay, suggesting that active pores were formed after g3p had been added to the aqueous phase probably due to the concomittant dilution of SDS upon sample addition to the aqueous phase. To test for this possibility, a 1% SDS-containing stock solution of monomeric g3p was diluted 1 : 100 into water and allowed to stand at 4°C for 24 h. Only 2.5–10 ng of the diluted monomer was sufficient to induce current jumps within minutes after addition to the aqueous phase. The addition of the same amount of protein from the stock solution to the aqueous phase did not induce any current jumps within an hour.

Cross-linking of native g3p

In order to determine the number of polypeptide chains associated within the g3p-oligomer, the Superose 12 column was calibrated with standard proteins the molecular masses of which ranged from 17 to 200 kDa. Calculated from linear regression (correlation coefficient: 0.986) original g3p exhibited a molecular mass of 62 kDa, whereas the molecular mass displayed by oligomeric g3p was calculated to be 194 kDa. This value fits very closely to the one expected for a trimer, which is 186 kDa. The same result was obtained if calibration of the column was with bovine liver glutamate dehydrogenase-monomer (56 kDa), -dimer, and -trimer. (Fig.

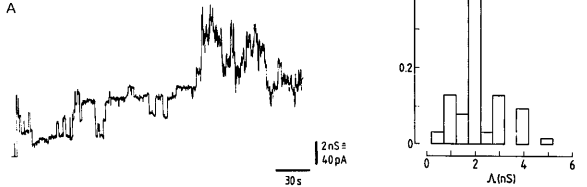

Fig. 5. Pore-formation observed with monomeric g3p. The aqueous phase was 1.0 M KCl. The membrane consisted of oxidized cholestrol/*n*-decane. (A) Single-channel recordings in the presence of 0.4 μg/ml g3p-monomer. The final SDS-concentration was 5 μg/ml. The applied voltage was 20 mV. (B) Histogram of the conductance fluctuations (see Fig. 4B for details). The average single-channel conductance was 2.1 nS ($n = 61$); the applied voltage was 100 mV.

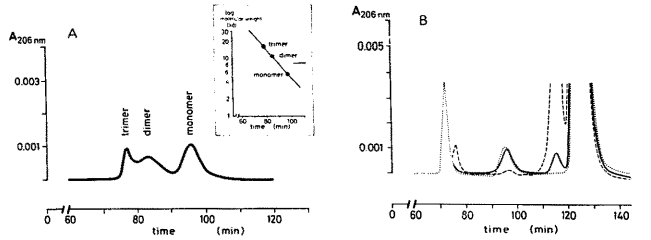

Fig. 6. Determination of the relative molecular mass of oligomeric g3p using a 'calibrated' Superose 12 column. (A) Calibration of the Superose 12 column using cross-linked bovine liver glutamate dehydrogenase. The inset displays the linear dependence of retention time on the relative molecular masses (as determined by SDS-gel electrophoresis) of the monomeric, dimeric and trimeric species. (B) Elution profile of equivalent amounts of native phage (·····), DTBP-treated phage (- - - - -), and DTBP-treated phage after reductive cleavage of the cross-linker (———). Phages were dissociated with SDS and their DNA partially separated prior to chromatography (flow rate 0.1 ml/min).

6A). The dimer and trimer were obtained by cross-linking native hexameric glutamate dehydrogenase (0.5 mg/ml) with dimethyl adipimidate (0.2 mg/ml) and their molecular mass determined by SDS-gel electrophoresis [37]. These results suggest strongly that the g3p-oligomer is composed of three subunits.

The adsorption complex of Ff-phages was reported to contain between 3 and 5 g3p molecules [4,31,33,35]. Assuming that in phage infection these g3p molecules form an oligomeric pore upon being inserted in the outer membrane, the number of g3p molecules in the adsorption complex should be the same as the number of g3p subunits in the pore. Therefore, native phage-associated g3p was cross-linked by treating native phage filaments with the cleavable imidoester DTBP. After cross-linking, phages were dissociated, the bulk of their DNA was sedimented by centrifugation and the resulting supernatant was analyzed on a Superose 12 column. Fig. 6B shows a comparison of the elution profiles resulting from equivalent amounts of untreated phage, DTBP-treated phage, and DTBP-treated phage after reductive cleavage of the cross-linker. Following DTBP-treatment, typically 50-100% of the monomeric g3p-peak disappeared in favour of a new peak. That this peak was intermolecular crosslinked g3p was confirmed by cleavage of the cross-linker which quantitatively transformed this peak into the g3p-monomer peak. The elution volume of cross-linked g3p was identical with that of the reassociated g3p-oligomer. This result suggests that it consists of 3 g3p-molecules. Cross-linked g3p-aggregates exhibiting higher molecular masses than the presumed g3p-trimer have not been detected. As the dimer was either not detected at all (Fig. 6B) or only in minute quantities relative to the trimer, we conclude that each phage filament contains three g3p molecules in a symmetrical arrangement.

Discussion

In this paper we describe a simple and efficient method for the purification of the adsorption protein of filamentous phage fd. G3p is isolated from SDS-dissociated fd-phage by gel-filtration using an FPLC-column in less than 2 h. The purified protein was homogeneous as judged by electrophoresis, rechromatography and amino acid analysis. SDS-treatment of phage liberates g3p as monomers. This is concluded from the fact that its elution volume did not decrease upon boiling of phage in 5% SDS under reducing conditions. Purified g3p which had been lyophilized after exhaustive dialysis to remove SDS was extremely difficult to solubilize and required sonication in 1% SDS. Following this treatment typically at least 50% of the g3p had aggregated into a discrete oligomer. We therefore suggest that the removal of SDS from monomers caused an exposure of lipophilic domains and their spontaneous oligomerization. The fact that monomeric g3p associated to predominantly one type of oligomer indicates that this oligomer is not an artefact but may be of functional significance.

The oligomeric form of g3p shares many properties characteristic of porin trimers from *E. coli*. It is stable under reducing conditions and in SDS. On the other hand, oligomeric g3p dissociates in SDS-gel electrophoresis whereas porins (without prior boiling) migrate as trimers [38]. Similar to porin trimers, the g3p oligomer inserts readily into lipid bilayer membranes to form membrane pores. However, the pores observed with

oligomeric g3p behave differently from those observed with porins: (i) their average lifetime is about two orders of magnitude lower. (ii) Downward directed steps or channel closing events are frequent, whereas with porins they are very rare. (iii) The single-channel conductance of the g3p-oligomer is 60–100% higher than those of the major *E. coli* porins OmpF or OmpC [27]. (iv) The current trace became increasingly noisy with the number of pores in the membrane so that hardly more than five pores at a time could be observed within a membrane. With porins more than 30 pores at a time have been observed [26].

The addition of oligomeric g3p to the aqueous phase would induce pore-formation within minutes. A similar delay is observed with porins and is explained by a diffusion of the protein to the membrane [27]. In contrast, pore-formation with the g3p-monomer under otherwise identical conditions was delayed for about an hour. This indicates that the monomer does not have pore-properties by itself. The delay may be explained by a diffusion of g3p monomers to each other and their refolding in secondary, tertiary and quarternary structure thereby forming an oligomeric pore-forming entity. This process seems to be induced by a reduction in SDS concentration upon sample dilution into the aqueous phase. This view is also supported by the finding that small amounts of monomeric g3p (2.5–10 ng) which had been diluted 1:100 into water 24 h prior to addition to the aqueous phase were capable of inducing current steps within minutes. However, if the same amounts of g3p-monomer were added from a stock solution in 1% SDS, a spontaneous occurrence of current steps could not be observed.

The distribution of pore sizes observed with monomeric g3p was wider than with oligomeric g3p. The wide size distribution reflects the existence of heterogeneous pores which could result from different conformations and numbers of subunits in the pore.

We therefore suggest that an oligomerization of g3p monomers is a prerequisite for pore formation and that the oligomeric form of g3p is the pore-forming entity.

Theoretical considerations also support an oligomeric structure of the pore. The conductance of the pores observed with g3p is extremely large. The predicted number of putative membrane-spanning domains in each monomer would probably not be enough to form a pore of this diameter [30,39]. Assuming that the A-protein pore is a wide water-filled pore similar to those of the porins from *E. coli*, *Salmonella typhimurium*, and *Pseudomonas aeruginosa* [27] its diameter can be roughly estimated. Provided that the pores are filled with a solution of the same specific conductivity, δ, as the external radius, r, and that the minimum pore length, l, is about 7.5 nm (which corresponds to the thickness of the membrane), the single-channel conductance is given by Benz [27]: $\Lambda = \Delta\pi r^2 \cdot l^{-1}$. By using the average single-channel conductance $\Lambda = 3.0$ nS in 1 M KCl and $\delta = 110\ \mathrm{mS \cdot cm^{-1}}$, the pore radius is calculated to be around 0.81 nm. For the OmpC- and OmpF-pore, respectively, a radius of 0.5 and 0.6 nm has been estimated [27]. Finally, cyclic symmetry seems to be a fundamental aspect in the design of membrane pores and channels.

The primary structure of g3p contains several putative membrane-spanning segments. However, their distribution among the amino acid sequence is uneven; they are either found towards the N-terminus or towards the C-terminus, whereas a long central domain which is flanked by the two glycine-rich sequences does not contain any of them (Fig. 1B). This central domain is relatively rich in proline and does not show any homology to the g3p of the related filamentous phage IKe which has a different receptor specificity [40]. That is why we propose that this domain is not involved in pore-formation but may represent the receptor-binding domain which is exposed as a knob on the phage. The two domains aminoterminal from the first glycine cluster and carboxyterminal from the second glycine cluster are potentially able to interact with the membrane and may be involved in pore formation. Upon membrane insertion of g3p, the central domain would presumably project into the aqueous phase. Alternatively, it might be buried in the pore interior or flip in and out of it, thereby closing and opening the pore. The 'noise' typical for current records with membrane inserted g3p might thus be explained by the presence of a domain not fixed in the membrane.

Gel filtration suggests that both the g3p oligomer and the adsorption complex at the tip of the phage consist of three g3p-molecules each. However, these results are only an estimate because gelfiltration in SDS has the following drawbacks: The hydrodynamic sizes measured are those of the SDS-protein complexes; these are not globular and the amount of SDS bound to g3p and the protein standards is unknown. In particular, g3p may bind different amounts of SDS in its monomeric, oligomeric and cross-linked form. As a consequence the hydrodynamic parameters may not be additive. On the other hand, we got the same results by using two sets of standard proteins. Also, a value of three g3p-molecules per phage is in agreement with our own unpublished results and with electronmicrographs of the fd adsorption complex which consistently reveal three 'knobs' at the tip of the phage [4].

In spite of the limitations of our approach it is tempting to hypothesize that the arrangement of the g3p-molecules in the adsorption complex reflects the symmetry of the g3p subunits in the pore. Based on this assumption we suggest the following model for the initial events in Ff-infection. After binding to the tip of an F-pilus and subsequent pilus retraction the adsorbed phage comes into contact with the bacterial outer mem-

brane. The initial contact between g3p and the membrane initiates conformational changes in g3p which bring about membrane insertion and oligomerization of the phage g3p-molecules. This process creates a membrane pore, thus allowing DNA-penetration through the outer membrane. The estimated radius of the g3p-pore (0.81 nm) is in agreement with such a function, the radius of the fd DNA-helix being 0.85 nm [41]. Our model is further supported by the findings of Jazwinski [10] and Marco [11] who demonstrated a quantitative uptake of phage g3p by infected cells. Also, incorporation of the integral phage g3p into the outer membrane was shown by Pelzer-Reith [12].

Further transfer of the DNA through the cytoplasmic membrane requires the products of the tolQRA gene cluster [13,14,42] and therefore presumably proceeds by a different mechanism.

Acknowledgement

We thank Dr. R. Benz for valuable advice with the lipid bilayer experiments.

References

1 Rasched, I. and Oberer, E. (1986) Microbiol. Rev. 50, 401–427.
2 Caro, L.G. and Schnoes, M. (1966) Proc. Natl. Acad. Sci. USA 56, 126–131.
3 Armstrong, J., Perham, R. and Walker, J.E. (1981) FEBS Lett. 135, 167–172.
4 Gray, C.W., Brown, R.S. and Marvin, D.A. (1981) J. Mol. Biol. 146, 621–627.
5 Boeke, J.D. and Model, P. (1982) Proc. Natl. Acad. Sci. USA 79, 5200–5204.
6 Davis, N.G., Boeke, J.D. and Model, P. (1985) J. Mol. Biol. 181, 111–121.
7 Burke, J.M., Novotny, C.P. and Fives-Taylor, P. (1979) J. Bacteriol. 140, 525–531.
8 Jacobson, A. (1972) J. Virol. 10, 835–843.
9 Marvin, D.A. and Hohn, B. (1969) Bacteriol. Rev. 33, 172–209.
10 Jazwinski, S.M., Marco, R. and Kornberg, A. (1973) Proc. Natl. Acad. Sci. USA 70, 205–209.
11 Marco, R., Jazwinski, S.M. and Kornberg, A. (1974) Virology 62, 209–223.
12 Pelzer-Reith, B. (1984) Ph.D. Thesis, University of Konstanz, F.R.G.
13 Sun, T.-P. and Webster, R.E. (1986) J. Bacteriol. 165, 107–115.
14 Russel, M., Whirlow, H., Sun, T.-P. and Webster, R.E. (1988) J. Bacteriol. 170, 5312–5316.
15 Lazdunski, C.J. (1988) in Membrane Biogenesis (Op den Kamp, J.A.F., ed.), pp. 375–393, Springer Verlag, Berlin.
16 Jakes, K.S., Davis, N.G. and Zinder, N.D. (1988) J. Bacteriol. 170, 4231–4238.
17 Lau, C. and Richards, F.M. (1976) Biochemistry 15, 3856–3863.
18 Ohno-Iwashita, Y. and Imahori, K. (1980) Biochemistry 19, 652–659.
19 Suzuki, K. and Imahori, K. (1978) J. Biochem. 84, 1021–1029.
20 Kornberg, A. (1974) DNA Synthesis, pp. 239–255, W.H. Freeman and Company, San Francisco.
21 Miller, J.H. (1972) Experiments in Molecular Genetics, Cold Spring Harbor Laboratory, Cold Spring Harbor, New York.
22 Yamamoto, K.R. and Alberts, B.M. (1970) Virology 40, 734–744.
23 Berkowitz, S. and Day, L. (1976) J. Mol. Biol. 102, 531–547.
24 Laemmli, U.K. (1970) Nature 227, 680–685.
25 Morrissey, J.H. (1981) Anal. Biochem. 117, 307–310.
26 Benz, R., Janko, K., Boos, W. and Laeuger, P. (1978) Biochim. Biophys. Acta 511, 305–319.
27 Benz, R. (1985) CRC Crit. Rev. Biochem. 19, 145–190.
28 Beck, E. and Zink, B. (1981) Gene 16, 35–58.
29 Mizuno, T., Chou, M.-Y. and Inouye, M. (1983) J. Biol. Chem. 258, 6932–6940.
30 Vogel, H. and Jaehnig, F. (1986) J. Mol. Biol. 190, 191–199.
31 Goldsmith, M.E. and Konigsberg, W.H. (1977) Biochemistry 16, 2686–2694.
32 Segawa, K., Ikehara, K. and Okada, Y. (1975) J. Biochem. 78, 1–7.
33 Woolford, J.L., Steinman, H.M. and Webster, R.E. (1977) Biochemistry 16, 2694–2700.
34 Simons, G.F.M., Konings, R.N.H. and Schoenmakers, J.G.G. (1979) FEBS Lett. 106, 8–12.
35 Lin, T.-C., Webster, R.E. and Konigsberg, W. (1980) J. Biol. Chem. 255, 10331–10337.
36 Simons, G.F.M., Konings, R.N.H. and Schoenmakers, J.G.G. (1981) Proc. Natl. Acad. Sci. USA 78, 4194–4198.
37 Hucho, F., Rasched, I. and Sund, H. (1975) Eur. J. Biochem. 52, 221–230.
38 Rosenbusch, J.P. (1974) J. Biol. Chem. 249, 8019–8029.
39 Spach, G., Heitz, F. and Trudelle, Y. (1983) in Physical Chemistry of Transmembrane Ion Motions (Spach, G., ed.), pp. 375–383, Elsevier/North-Holland, Amsterdam.
40 Bross, P., Bussmann, K., Keppner, W. and Rasched, I. (1988) J. Gen. Microbiol. 134, 461–471.
41 Banner, D.W., Nave, C. and Marvin, D.A. (1981) Nature 289, 814–816.
42 Sun, T.-P. and Webster, R.E. (1987) J. Bacteriol. 169, 2667–2674.
43 Capaldi, R.A. and Vanderkooi, G. (1972) Proc. Natl. Acad. Sci. USA 69, 930–932.
44 Kyte, J. and Doolittle, R. (1982) J. Mol. Biol. 157, 105–132.